Geophysical Prospecting 32, 608–628, 1984.

VSP INTERVAL VELOCITIES FROM TRAVELTIME INVERSION*

R.R. STEWART**

ABSTRACT

STEWART, R.R. 1984, VSP Interval Velocities from Traveltime Inversion, Geophysical Prospecting 32, 608–628.

A principal use of the vertical seismic profile (VSP) is to determine the variation of seismic velocity with depth. Presented here is a discussion of the errors involved with the time picks of a VSP survey and several methods currently used to calculate a velocity section from these time picks. Another technique is proposed, based on the least-squares inversion of the traveltimes, to arrive at a better estimate and statistical description of the velocity section. This technique uses the Levenberg–Marquardt damped least-squares formulation and ray tracing through a horizontally-layered medium to iteratively refine the velocity section. The accuracy and robustness of the procedure are investigated by inverting noisy traveltime curves and comparing these results to the original model velocity section. Agreement is found to be good. One interesting feature of the inverse procedure is that, for certain geometries, it can resolve a few velocity layers, even though there are no measurements made inside those layers. Three actual VSP surveys are analyzed and compared to their corresponding sonic logs. In two of the surveys, it appears that there is some velocity dispersion. Velocity changes associated with gas saturation are evident on one of the surveys.

INTRODUCTION

Vertical seismic profiling (VSP) is becoming increasingly recognized as a valuable technique in seismic exploration (Gal'perin 1974, Kennett, Ireson and Conn 1980, Stewart, Turpening and Toksoz 1981, Balch, Lee, Miller and Ryder 1982, Hardage 1983). Perhaps the most basic information inferred from the VSP is the variation of seismic velocity with depth. Because of this, it is necessary to develop and use methods by which the velocity section may be calculated in an accurate and reliable manner. Currently, some classical techniques are being employed (Dix 1945, Grant and West 1965). These methods all use first arrival times picked from the VSP traces. Thus, the VSP is being considered as a dense check shot survey. Simple assumptions are made concerning the ray propagation paths to calculate a velocity

* Received January 1983, revision November 1983.

** Department of Earth, Atmospheric and Planetary Sciences, MIT, Rm 54-510, Cambridge, MA 02139, USA, currently at Chevron Geosciences Co., 500 Fifth Ave. SW, Calgary, Alb. T2P 0L7, Canada.

section. In only a few studies have the limits and errors inherent in the VSP observations and velocity calculation been considered (Gamburtsev 1969, Beeston and McEvilly 1977, Goetz, Dupal and Bowles 1979).

This paper describes the methods and assumptions involved in several techniques presently used to process VSP traveltime data. Some of the errors associated with a VSP survey and the problems that these pose for analysis techniques are considered. To solve some of these difficulties and to allow quantitative estimation of the quality of the solution, while still limited to traveltimes, another technique is proposed. It is based on a damped least-squares linear inverse algorithm which simultaneously determines all interval velocities from the traveltime data.

The inverse algorithm is tested by application to synthetic data. These are generated by ray tracing through a model velocity section. Next, noise is added to the traveltimes determined from this ray tracing. The inverse algorithm then inverts the noisy traveltime data to arrive at a velocity structure. This calculated velocity section is compared to the original model velocity section.

Three field VSP examples (all land surveys) are analyzed for velocity and are compared with the corresponding sonic logs. An attempt is made to use the inversion results to constrain the velocity layer thicknesses. The results are also used to determine lithological boundaries.

Current Techniques

There are two simple approaches to the calculation of velocity from VSP traveltime data. It is possible to use the traveltime differences from a single source to different depths to compute an interval velocity (Dix 1945, Grant and West 1965). Alternatively, the traveltimes from a number of surface source offsets to a fixed receiver at depth can be used to find an RMS velocity corresponding to that depth from the move-out curves (Dix 1981). This second method is only rarely used, partially due to the expense of the many source offsets required to adequately define the moveout curves. Shooting up-hole (sources in the well with a surface spread of receivers) is the reciprocal of the previous techniques (Gal'perin 1974, Alam, personal communication 1981). This up-hole method is also used only occasionally and then at the near surface because of down-hole source size limitations. Tomographic-type interpretation schemes for multiple source offsets have been proposed (Devaney 1982) and field work attempted (MIT/CGG 1983). Stewart (1983) and Grivelet (in a paper read at the 53rd SEG Meeting, Las Vegas 1983) have also outlined inversion schemes using the full waveform. In the future, these alternate methods will no doubt become more widely used than they are now.

Considered here is only the routine single source offset case. The basic data set upon which all current analysis methods operate is the traveltime-versus-depth curve. The time-versus-depth curve is determined from a trace section by picking the first-arriving energy. By using only the first arrival in the VSP trace, a great deal of information in the later part of the trace is being neglected. This is usually justified by noting that the first arrival has the best signal-to-noise ratio (at least 20 dB higher than the primary reflection) and represents the most straightforward wave type: the direct wave. Pulse height detection, eye picking or trace cross-correlation are all methods by which the first-arrival times may be deduced. A comparison of these different picking methods is discussed by Stewart, Huddleston and Kan (1983). They found interactive cross-correlation to be the preferred technique.

The differences in the techniques for computing the velocity structure lie in the assumptions made about the ray path of the propagating energy. The simplest assumption is that the ray travels strictly vertically from the source to the receiver. This approximation is equivalent, in velocity terms, to finding an interval velocity (the apparent velocity) by differentiating the traveltime curve.

$$\text{apparent velocity} = (\Delta t/\Delta z)^{-1}, \tag{1}$$

where Δz is the depth interval between stations and Δt is the difference in traveltimes measured at these stations.

The usual correction applied to this vertical ray path is to assume that the ray travels in a straight line from the offset source to the receiver (Lash 1980). This gives a slanted-straight-ray velocity

$$(\Delta z/\Delta t) \cdot \cos \Theta, \tag{2}$$

where Θ is the angle subtended by the line from receiver to wellhead and receiver to shot points.

Now assume that rays propagate through discrete flat-lying layers, bending at each interface in accordance with Snell's law. Grant and West (1965) derive a relation between the velocity structure and traveltimes. They show that the total traveltime T, to some depth H, is related to the velocity structure $V(z)$, and traveltime derivative $\mathrm{d}T/\mathrm{d}z$ as follows:

$$T(H) = \int_0^H \left\{1 - V^2(z)\left[\frac{1}{V^2(H)} - \left(\frac{\mathrm{d}T}{\mathrm{d}z}\right)_H^2\right]\right\}^{-1/2} \frac{\mathrm{d}z}{V(z)} \tag{3}$$

Supposing that $T(H)$ and its derivative $(\mathrm{d}T/\mathrm{d}z)_H$ have been measured, then (3) may be numerically integrated to determine $V(z)$. This is done by first solving (3) for the surface layer, then the next layer and so on. This boot-strapping process is repeated until the complete velocity section has been calculated. Equation (3) does require a search for the velocity $V(H)$ in each layer. A rapid search algorithm (after Bickle, personal communication) has been incorporated into the program to calculate velocities using (3).

To test briefly the validity of these different methods, synthetic traveltime curves are generated (by offset one-dimensional ray tracing) for a known velocity section. These traveltime curves are processed by the three preceding techniques. The model velocity section and the results for the apparent and straight ray velocities are shown in fig. 1. As may be expected, especially at shallow depths and high velocities, these two methods give poor estimates of the true interval velocities.

The ray trace approach gives much better results. Figure 2 shows the model velocity with the velocities computed from ray trace integral using the traveltime data as in fig. 1. The agreement is good, as expected, since the model traveltimes are ray trace generated, and (3) is based on ray tracing. This suggests that for these noise free data at least, the VSP velocity problem is well-behaved and invertible.

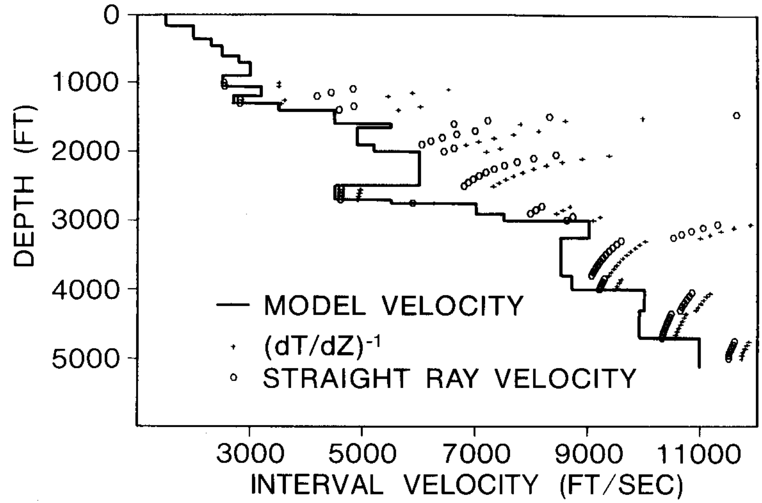

Fig. 1. Model velocity section and velocities calculated using vertical rays (apparent velocity) and slanted straight ray assumptions. The deeper velocity estimates are more valid, as the assumed and actual rays are both nearly vertical. In the shallow section, the actual rays are more horizontal than the assumed rays. Source offset is 300 m (1000 ft).

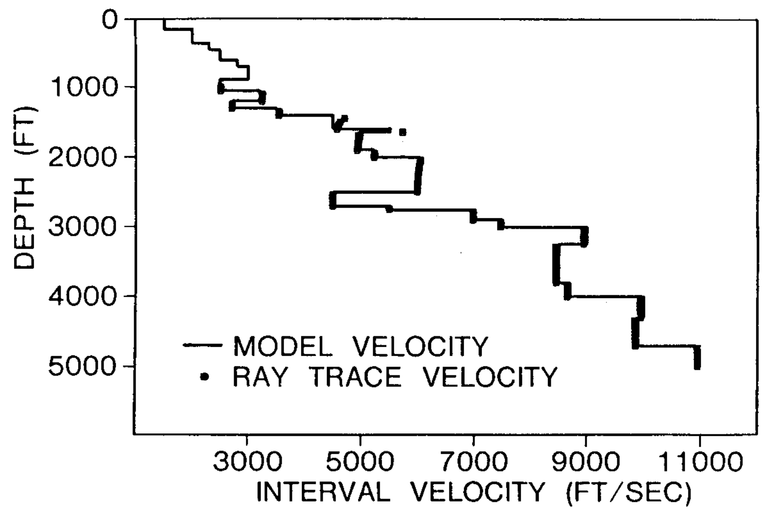

Fig. 2. Velocities calculated from the traveltimes from fig. 1 using the ray path integral, equation (3).

Figure 3, from Grant and West (1965), shows another velocity comparison for the different ray path assumptions. There are large discrepancies between the velocity estimations from the same traveltime data. Note that the ray trace integral gives unlikely velocities of about 9000 m/s near the 2130 m/s depth. It appears that the ray trace integral inverts synthetic data well, but has some difficulty processing real data with errors or noise. Errors involved in a VSP survey must be considered.

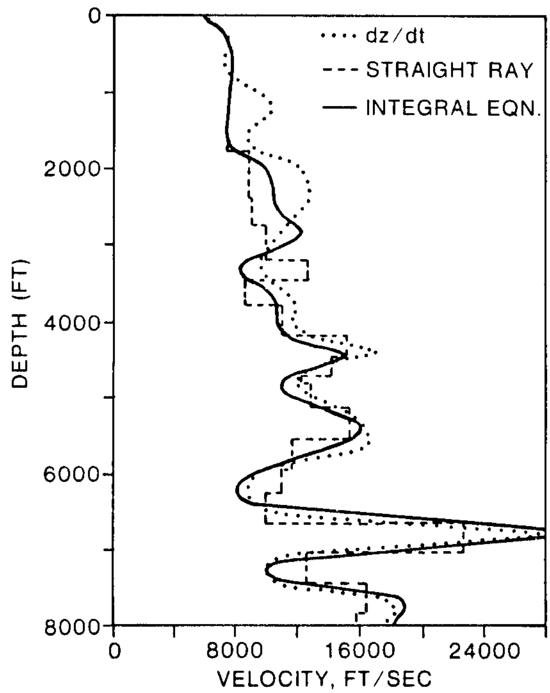

Fig. 3. A VSP performed in Louisiana and analyzed by Grant and West (1965). Source offset was 300 m (1000 ft). Three velocity estimates are plotted using the ray path assumptions underlying equations (1), (2) and (3). The differences in these velocities are quite substantial. Note the unrealistic velocities at about 2130 m (7000 ft).

Attempting to define the error associated with an observation is an arduous and generally unpleasant task. Yet understanding the errors in a survey will help define the accuracy of the calculated velocities. Two fundamental observations in the VSP survey are the total traveltimes from source to receiver and the depth of the receiver.

The true depth of the receiver is approximately known but difficult to specify exactly (Zeitvogel 1982). Depth precision or repeatability is often claimed to be on the order of several tenths of a foot. But slippage of the tool in the well, without re-recording the final depth, could easily result in depth errors of several feet. This slippage is probably systematic throughout the survey, as the tension on the cable is customarily reduced after clamping the tool (this procedure is designed to reduce cable wave propagation). The actual depths then, are probably systematically several feet deeper than thought. Random errors, such as operator error, cable stretching, and tool movements while clamping, probably introduce another several feet inaccuracy*. This means that the time error, due to the random depth inaccuracies, is about 0.5 ms (for an interval velocity of 1830 m/s).

The errors involved in estimating the traveltimes are due to inaccurate time picking, inexact zero times, and instrument imprecision. Goetz et al. (1979) suggest that the instrument errors can be of the order of 1.0 ms. In general, the instrument errors are systematic delays and either cancel out in interval velocity calculations or at most provide a small shift to the shallow velocities (as do systematic tool slippage errors). Gamburtsev (1969), in a series of shallow experiments, estimates the standard deviation of the P wave total traveltime to be 0.5 ms. Beeston and McEvilly (1977) also suggest that timing estimates are accurate to ± 0.5 ms (see Appendix A for picking error analysis). Adding these to the previously determined depth error (converted to time) gives an approximate total time error of about ± 1.5 ms. Stewart et al. (1981) find maximum errors in a detailed Michigan VSP to be 2.0 ms for P waves and 3.0 ms for S waves. Very carefully executed surveys may have somewhat higher precision than the above estimates.

A more subtle type of error is associated with wave propagation effects. Short-path multiples may cause small delays in the seismic traveltimes. This effect is significant in only highly cyclically-stratified sections where it may induce seismic delays of about 2.0 ms/300 m with respect to the sonic log (O'Doherty and Anstey 1971, Schoenberger and Levin 1978, Stewart et al. 1983). If a cyclically-stratified section is suspected, this drift could be subtracted prior to analysis. Otherwise it will be largely negligible.

Assuming a simple geometry, it is possible to calculate the effect of a given time error Σ_t, on an interval velocity. If a plane wave is incident on two vertically-spaced receivers then the following worst case estimate can be computed for the error in velocity Σ_v:

$$2\Sigma_v = \frac{\Delta z \cos \Theta}{t_1 - t_2 - 2\Sigma_t} - \frac{\Delta z \cos \Theta}{t_1 - t_2 + 2\Sigma_t}, \tag{4}$$

where Δz is the interval between recording stations, $\cos \Theta$ is the cosine of the incidence angle, t_1, t_2 are the traveltimes to receiver positions 1 and 2, and $\Delta t = t_1 - t_2$. Letting the velocity of the medium be $V = \Delta z \cos \Theta / \Delta t$ and inserting this into (4) and assuming that $\Sigma_t/\Delta t$ small gives the relative velocity error

$$\frac{\Sigma_v}{V} = \frac{2\Sigma_t}{\Delta t}. \tag{5}$$

* A British geophysicist related the following story at the 1981 SEG meeting: he and his colleagues were atempting to conduct an offshore VSP but were recording a great deal of noise with little signal. After many frustrating minutes, they realized that the tool was still on the deck and not in the hole at all. Such depth errors are difficult to quantify.

If $\Sigma_t = 1.5$ ms, $\Delta t = 6.0$ ms—a depth interval of 15 m for a velocity of 2500 m/s—then the relative error in velocity is 50%! Evidently, time errors play a major role in the determination of an interval velocity.

Mismatches between noisy field observations and calculated values will still occur to an extent sometimes even greater than the errors predicted above. This is due to the simplified horizontally-layered earth model and one-dimensional ray tracing. Thus, there is error in the analysis techniques as well as the observations.

By adding random perturbations to synthetic traveltimes, it is possible to directly investigate the effect of the observation errors on the computed velocity. In particular, the synthetic times from the velocity section of fig. 1 are used. The error or noise added to those times has been pseudo-randomly distributed between -1.0 ms and 1.0 ms. One of these random errors has been added to each traveltime point. This results in a perturbed traveltime-versus-depth curve. This curve is inverted using (3). The scatter in velocities so determined is evident in fig. 4. The scatter is greater in the deeper part of the section. This is due to the constant time error with decreasing time intervals between stations of constant depth difference (i.e., Σ_t is constant, while Δt becomes smaller). There is also the cumulative effect of inaccurate previous (more shallow) velocities.

To reduce traveltime scatter, and thus arrive at a smoother velocity estimate, different time averaging techniques have been used. For example, smoothing the noisy traveltime curve with a three point average, then inverting the data with the ray trace integral, results in a better velocity estimate. Perturbations larger than about ± 2.0 ms cause the algorithm to abort.

It is seen that computed interval velocities are very sensitive to the input traveltimes. The velocity accuracy may be enhanced by using averaging techniques on noisy data. However, a definite criterion for averaging is needed. It is not known, a

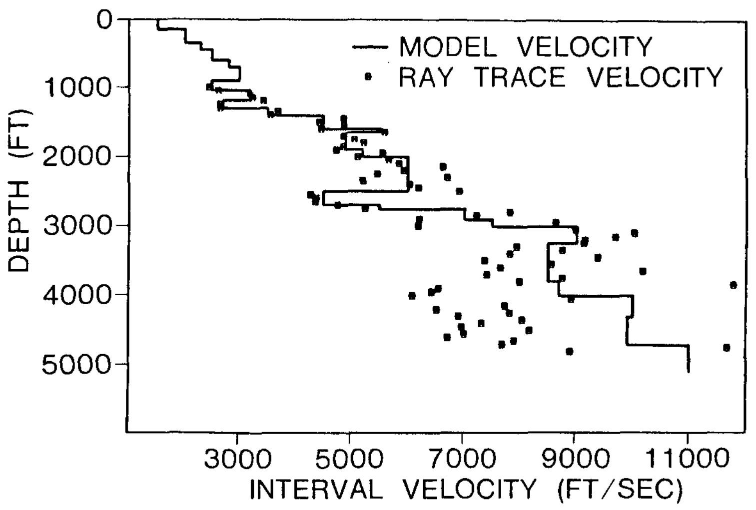

Fig. 4. Velocities calculated by the ray integral method from noisy travel times. The traveltimes are generated by ray tracing through the structure of fig. 1 with a 300 m (1000 ft) source offset. They are then mixed with random noise from -1.0 ms to 1.0 ms.

priori, how many points to average over and what type of averaging to use. Even if an average appears to work for the data, the quality of the solution is uncertain. Large errors can cause inaccurate velocities, which, if incurred in the shallow depths, perturb the rest of the section. This is a result of the bootstrapping nature of the algorithm. Large errors (>2.0 ms) cause the algorithm to abort. Thus, the previous techniques are operator intensive and require constant monitoring and interpretation.

Inverse Formulation

As mentioned above, current techniques have certain shortcomings. VSP data are expected to become increasingly complex, due to multiple source offsets with different depth intervals. To process all these data simultaneously and optimally is very difficult with present techniques. With a least-squares inverse method, though, multiple data sets can be processed as a matter of course (Rice, Allen, Gant, Hodgeson, Larsen, Lindsey, Patch, LaFehr, Pickett, Scheider, White and Roberts 1981). The following discussion is a brief description of the classic linear approach (Flinn 1960, Crosson 1976, Aki and Richards 1980, Thurber 1981).

In general, the inverse procedure is used to correct an initial guess at a number of parameters. In the VSP case, the first step is to ray-trace through an estimated velocity model. These calculated ray-traced traveltimes are compared (in a least-squares manner) to the observed field times. It is assumed that the difference between calculated and observed times (the "residual") is linearly related to the change that needs to be made in the velocity model. This change is calculated using inverse matrix methods. This process is repeated until either the difference in the observed and calculated traveltimes is within the experimental error or the velocity model is no longer changing significantly.

The traveltime problem is actually nonlinear (Wiggins 1972). Nonetheless, small changes in the velocity structure are approximately linearly related to the traveltime residual. Because only small changes are permitted, the process must be iterated to arrive at a final solution.

A useful statistical parameter to describe how well the parameters are constrained arises from the inversion process (refer to Appendix B for a discussion of the inverse formulation). The square root of a given diagonal element of the covariance matrix of the velocity changes is the error in the velocity parameters due to errors in the traveltime data.

Another quantity which is useful in examining the solution is the final traveltime residual. At every depth, the residual reflects the mismatch between the observed data and the calculated data. A single, large residual probably indicates an erroneous time. Several adjacent mismatches are often diagnostic of a poorly-defined velocity layer. For example, a thick model layer covering two distinct real velocity layers will have a velocity that is approximately the average of the two real layers. However, the layer will have a polarity change in the sign of the residuals associated with it. This is an indication that an insufficient number of layers have been used. These measures, the standard deviation, and residuals may be used to examine the quality of the solution.

The present inversion routine is operating on a mid-size computer system (VAX 11/780). It uses a standard ray tracing algorithm for horizontal layers and an offset source. A finite difference Levenberg–Marquardt matrix inversion subroutine (Marquardt 1963, Brown and Dennis 1972) performs the formal inversion. The next section describes the testing and usage of this inverse process on synthetic and real VSP data.

Inversion Results

Synthetically-generated data are used to test the algorithm. This determines the overall accuracy of the algorithm and the effect of noise on its stability. Also analyzed is the inversion of synthetic data that has some observation points missing. In particular, the top few observations are not used, but the velocity layers at these depths are kept. This leads to some interesting results.

Three field VSP data sets are analyzed and compared with the corresponding sonic logs.

Synthetic examples

A theoretical traveltime curve is generated by ray tracing through a model velocity section. Traveltime noise may be added to the curve. This perturbed curve is then processed using the inversion algorithm. Figure 5 shows the results of an inversion performed on the traveltimes of rays traced through the interval velocities of fig. 1 with a 76 m source offset. The velocities so determined are largely within one

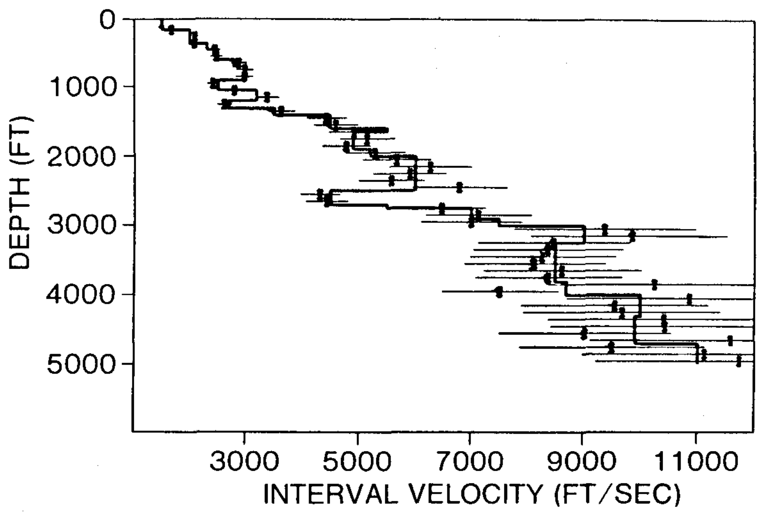

Fig. 5. Interval velocity versus depth as determined by the linear inverse. Noise (−1.0 ms to 1.0 ms) and interval velocities are the same as that of fig. 4 but the source is now offset only 76 m (250 ft). Horizontal bars indicate one standard deviation of velocity limits.

standard deviation of the model velocities. The velocities are closer to the model values than are the previous ray-trace integral results.

In the next case, a large amount of noise (randomly generated from -3.0 ms to 3.0 ms) was mixed with the traveltime curve. Figure 6 shows the results for layers parameterized at the same depth as the model layers. The velocity estimates are generally within two standard deviations at the deeper depths. In the shallow section, the velocities are usually within one standard deviation. Recall that the ray-trace integral method usually aborts when more than 2.0 ms noise is mixed with the traveltime data.

In a typical VSP survey, the top several hundred feet of data are often of low quality (if recorded at all). This is due to cultural noise, multiple casings, and complex wave propagation. It is desirable, then, to use only the deeper traveltimes to constrain the surface velocities. This possibility has been investigated, using the synthetic traveltimes. Once again, ray tracing through the velocity model yields traveltimes. To these times random noise was added from -1.0 ms to 1.0 ms. In this case the top 150 m of observations (which were taken every 8 m) were not used in the inversion. Two velocity layers were placed, nonetheless, in the top 150 m. The results of the inversion are given in fig. 7. Note that the model velocities in the top two layers are closely approximated by the inversion results. The small standard deviations indicate that the algorithm was able to constrain the velocities fairly well. Intuitively, this is understandable for several reasons. In the first place, there are still many more observations (180) than layer velocities (15). Because the source was offset 183 m, the upper two velocities have a large effect on the ray propagation direction and traveltimes to deeper observations. Thus, these lower observations include information on the upper layers. The inverse must find velocities for the upper layers to satisfy the observations in the deeper layers.

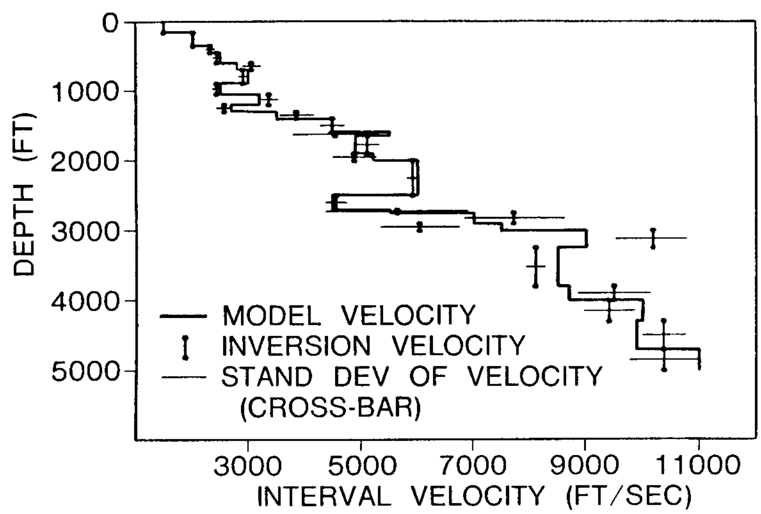

Fig. 6. Interval velocity versus depth from the linear inverse. Random noise from -3.0 ms to 3.0 ms is mixed with the traveltimes from fig. 1. These noisy data have been inverted.

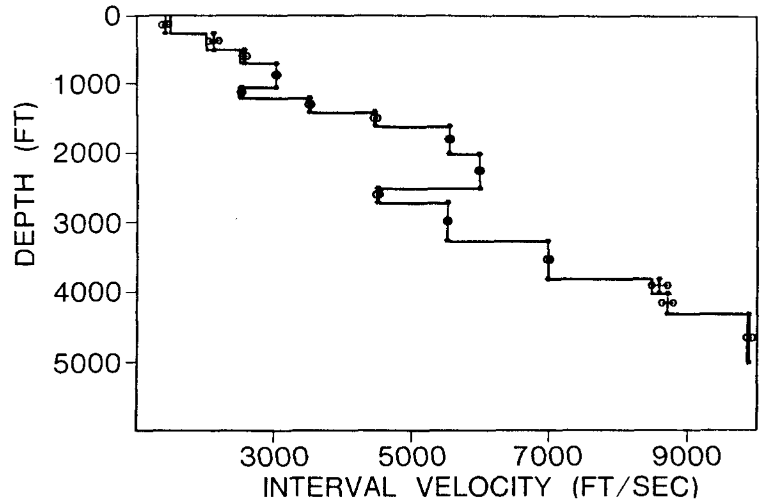

Fig. 7. Interval velocity versus depth from the linear inverse. Traveltimes are calculated through the velocity structure shown with a solid line. Random noise from −1.0 ms to 1.0 ms has been added to these times. The top 150 m (500 ft) of observations have been discarded and inverse performed. Note the small errors associated with the velocity estimate.

Gulf Coast VSP

This survey was performed in a cased well on the coast of Alabama. A slanted weight drop device positioned 79.6 m from the well-head was used to generate both P and right and left-polarized SH waves. The survey was recorded from the well bottom of 500 m to the surface, at 3 m receiver spacings with a three-component wall-clamping tool.

The well encountered only highly unconsolidated sediments. The top half of the section was mainly composed of silts and sands which trended into shale-sand interbedding for the lower half of the section. The sonic log (fig. 9) indicates that two gas sands were penetrated at (404–410 m) and (456–460 m) depths. Kicks on the drill string while drilling the well were evidence that the sands were highly pressurized with gas.

The traveltimes for P and SH waves were picked and put into the inversion routine using layer thicknesses of 12 m. The P velocity so determined is shown in fig. 8. The velocities are quite low (about 1800 m/s) due to the unconsolidated nature of the sediments. At 400 m there is evidence of gas sand. The velocity is dramatically lower both because of the sand and its high gas pressure (low differential pressure). Although 12 m layers were used, the velocity anomaly over the thin sand is quite visible. Generally, the VSP and sonic log show the same velocity trend, although in the top 300 m the VSP values are slightly lower than the sonic velocities. The VSP has several high (2440 m/s) velocities, which, judging by the magnitude of the error bars, are probably due to spurious traveltime values. These could be edited or weighted to be less significant.

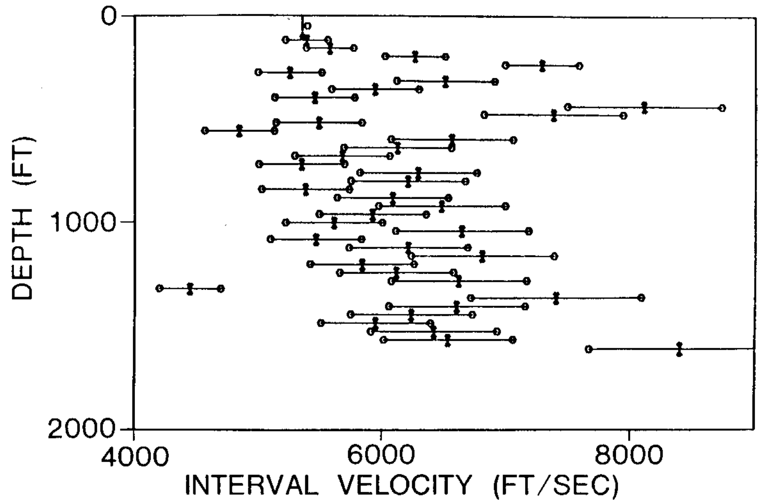

Fig. 8. P interval velocity versus depth for Gulf Coast well from linear inverse. The well below 488 m (1600 ft) was plugged with cement before the VSP was run. The depth interval between observations is 3 m (10 ft) and the velocity layers are 12 m (40 ft) thick. The P traveltimes were picked from the traces of the vertical geophones. The horizontal bars give the standard deviation of the velocity due to errors in the data.

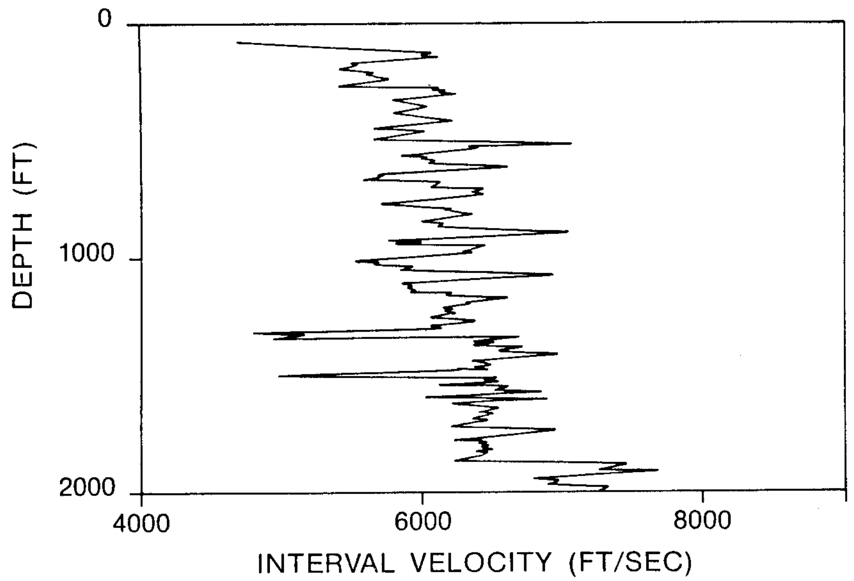

Fig. 9. Sonic log versus depth for Gulf Coast well. Note the two low velocity gas sands.

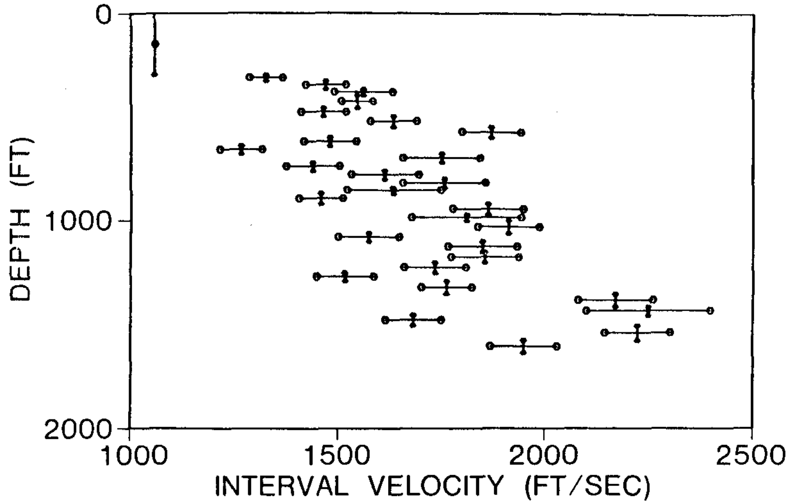

Fig. 10. SH interval velocity versus depth for Gulf Coast well from linear inverse. Observations were made every 3 m (10 ft). SH traveltimes were picked by overlaying left and right polarized shear wave traces (from the horizontal geophones). SH velocity increases with depth. The two low velocity gas sands are identifiable at about 400 m (1300 ft) and 460 m (1500 ft) depths. The horizontal bars give the standard deviation of the velocity due to errors in the data.

The SH velocities in fig. 10 show a greater trend with depth than the P velocities (Gregory 1977). The low velocity at 400 m is indicative of the high pressure gas sand. Interestingly, the SH velocity is significantly lowered at 457 m also. It appears that this thinner deeper gas sand has a larger effect on the SH waves than the P waves. This may be because the SH waves have a considerably shorter dominant wavelength than the P waves (about 30 m versus 60 m).

The V_p/V_s ratio was very high; it changes from a near-surface value of about 7.0 to a minimum of 3.6 at depth. Such high and variant ratios are a factor in making the correlation of P and S reflection surveys somewhat difficult.

Using the velocities measured in the upper gas sand $V_p = 1340$ m/s and $V_s = 466$ m/s gives a $V_p/V_s = 2.88$. This translates into a Poisson's ratio (σ) of 0.43. Nearby brine-saturated sediments have $V_p = 1950$ m/s and $V_s = 533$ m/s. This gives $V_p/V_s = 3.66$ and $\sigma = 0.46$.

Hydrostatic pressure at a depth of 405 m is about 40 bar (600 psi). Lithostatic pressure will be slightly higher (60) bar with a sediment density of 1.5 g/cm^3. Domenico (1977) thoroughly measured the elastic properties of the Ottawa sand (a fine-grained quartz sand). If the differential pressure is 20 bar his graphs indicate that $V_p \approx 1850$ m/s and $V_s \approx 550$ m/s in the saturated sediments. Poisson's ratio is about 0.45. These values are similar to those determined above.

The small traveltime residuals, reasonable velocity errors and correspondence of the VSP velocities to the sonic log indicate a good solution.

The final traveltime residuals for the P survey were less than 1.0 ms, while the S survey had residuals less than 2.0 ms. The error in the velocities due to the traveltime error for both cases is less than 10%.

For the previous cases, the inverse algorithm requires about five iterations for convergence to the final solution. This takes on the order of a minute of computer CPU time on the VAX system.

Numerous other layering-thicknesses were used in the SH inversions. For example, one case computed the velocity section for 6 m (20 ft) layers. The RMS value of the residuals was 0.6, but the errors were about 150 m/s (500 ft/s). Thus the attempted fine resolution produced excessive error.

ENIX VSP

A VSP was conducted in early 1980 in East Texas. Six Dinoseis guns were positioned 30 m away from the wellhead to perform the survey. Recordings were made with a wall-clamping three-component tool every 7.6 m from the well bottom at 663 m to the surface.

The geological section is composed primarily of Cretaceous and Tertiary sediments. Shales and limestones extend from the near surface to a depth of 238 m. From here, the Arkadelphia marl trends into the Nacatoch sandstone at 329 m. Below this is the Taylor Group (sandstone, shale, marl) to 610 m. This in turn is underlain by the Pecan Gap chalk.

Figure 11 shows the results of a traveltime inversion for 23 m thick layers. An

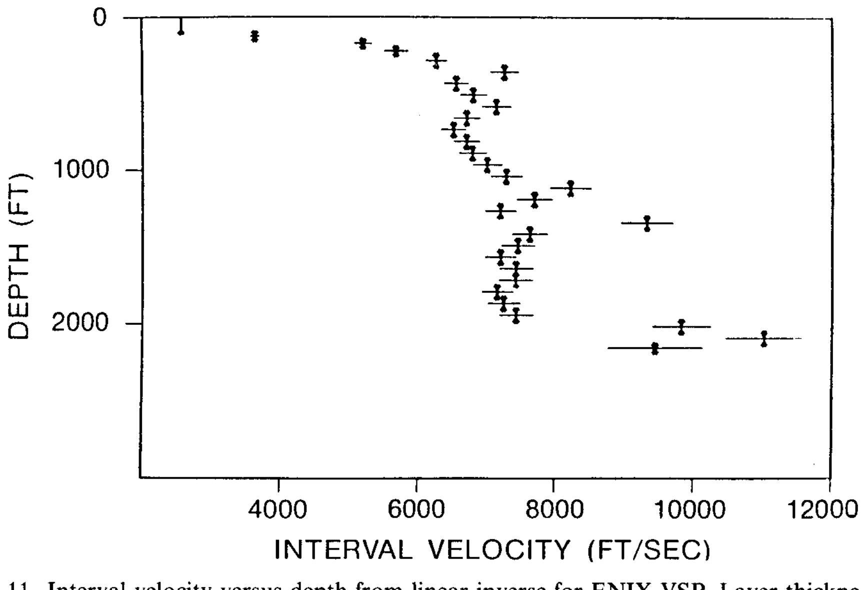

Fig. 11. Interval velocity versus depth from linear inverse for ENIX VSP. Layer thickness of 23 m (75 ft) are used. The depth between observations is 8.00 m (25 ft). A P traveltime is picked from the trace of the vertical component geophone at each level. The horizontal bars give the standard deviation of the velocity due to errors in the data.

inversion was also performed on a model with 30 m layers. The velocity estimates for the two cases were quite similar. However, some differences do exist. For example, on the 23 m layer model the next-to-bottom layer is bounded by lower velocities, whereas, on the 30 m layer case, there is but one layer. The lithological section indicates that there is, in fact, a high velocity chalk layer underlain by a slower marl.

From the sonic log (fig. 12), it is seen that while the overall trends of the sonic and VSP velocities are similar the VSP velocities are consistently lower. This area also has a high attenuation. A number of authors have proposed an association

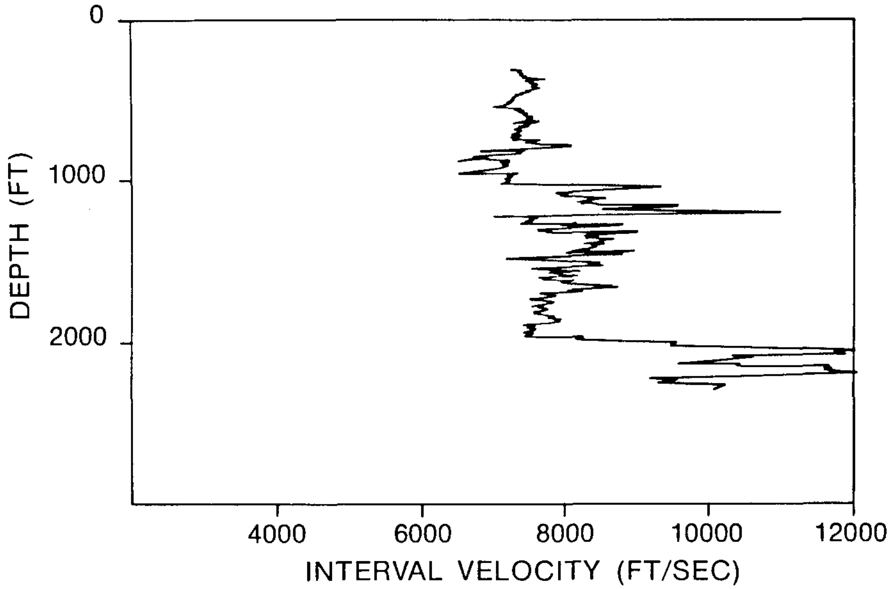

Fig. 12. Sonic log versus depth for ENIX well.

between attenuation and velocity dispersion (Wuenschel 1965, Strick 1971, Ganley and Kanasewich 1980; Stewart et al. 1983). In these models, the VSP velocities should be a few percent lower than the sonic velocities, as is observed above.

The standard deviation of the velocity (about 5% relative error) and small traveltime residuals (<1.0 ms) indicate a high quality survey and reasonable velocity model.

Colorado VSP

A thorough geophysical survey was conducted by ARCO Oil and Gas Company in Colorado. It included a full spectrum of logs and a VSP. The VSP was recorded in Well #100 from a total depth of 2246 m to 290 m at 23-m intervals. The survey used a group of four vertical vibrators offset at a distance of 300 m from the wellhead. A wall-clamping, three-component receiver provided good vertical but poor horizontal traces.

In this area, the geological section is largely composed of shale (Pierre and Niobrara) to a depth of 1250 m. From here to the bottom of the well there are alternating sandstones (e.g., Dakota), shales (Morrison), and limestones (Timpas). The Sangre de Cristo redbeds are encountered at 1638 m.

Figure 13 shows a thick layer (approximately 183 m) velocity interpretation of the Colorado VSP from the inverse algorithm. The traveltime residuals for this interpretation were rather large, often up to 2.0 ms, which was more than expected.

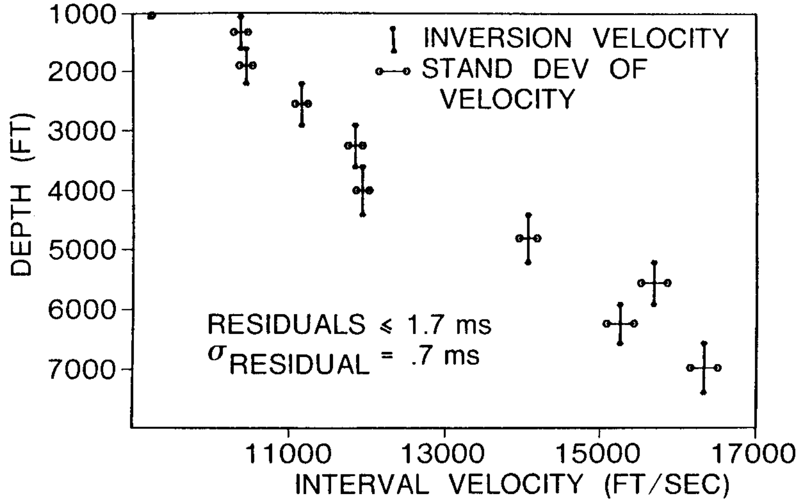

Fig. 13. P interval velocity versus depth for Colorado VSP (Well #100) from the linear inverse. Observations were made every 22.50 m (75 ft). The P traveltimes were picked from the vertical geophones. Velocity layers are 183–244 m (600–800 ft) thick. The horizontal bars give the standard deviation of the velocity estimate.

The RMS value of the residuals was 0.7 ms. The standard deviations of the velocities were quite small. These highly constrained velocities (with unrealistic standard deviations) indicated that the resolution was too poor (i.e., velocity layers are too thick). Accordingly, the model was reparameterized with thinner layers (45 m thick). In fig. 14, the results of the velocity inversion are shown. The high velocity redbeds are apparent at 1646 m. The standard deviations of the velocity were more realistic (6–10% relative error) and the traveltime residuals were around 1.0 ms. The standard deviation of all the residuals was 0.3 ms. Figure 15 is a plot of the unedited sonic log velocities. Note the scatter in the sonic log. While much of this scatter may be edited out, questions of accuracy still remain. The VSP velocities are less sensitive to, for example, borehole conditions and can give better constrained velocities. The shallow VSP velocities are somewhat lower than those of the sonic log as in the ENIX well. This is perhaps due to a higher attenuation in the shallow section which could be associated with velocity dispersion.

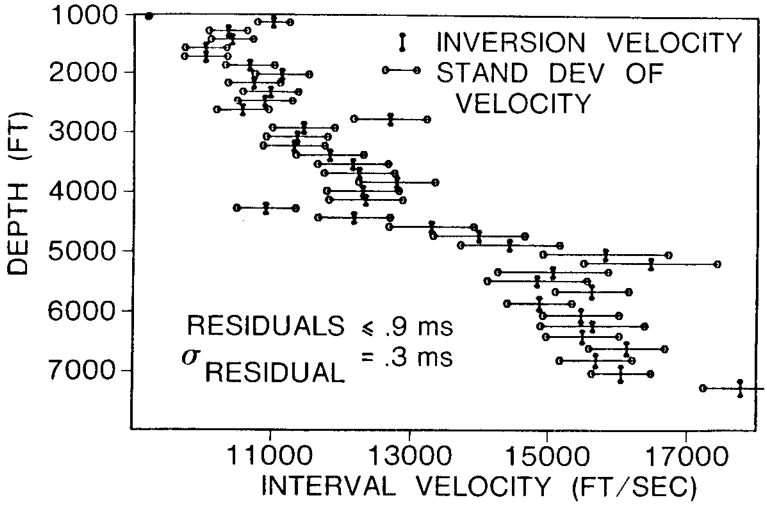

Fig. 14. P interval velocity versus depth for Well #100 as in fig. 15. Velocity layers are 45 m (150 ft) thick and standard deviations are shown.

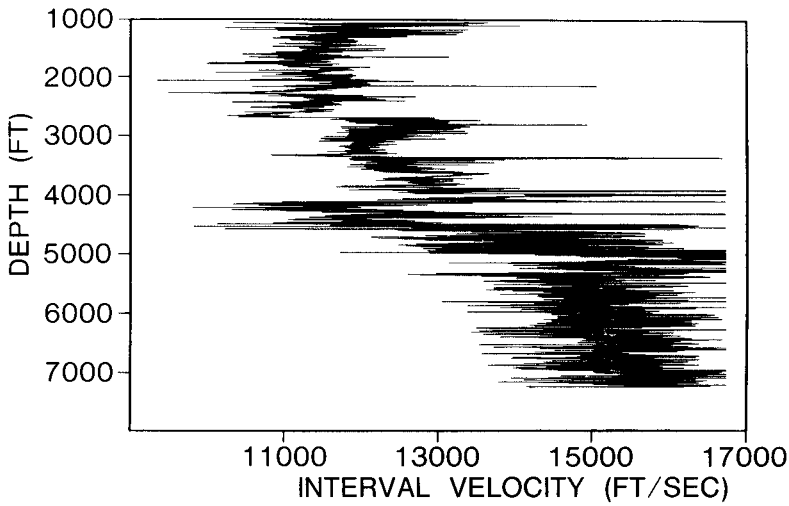

Fig. 15. Unedited sonic log versus depth for the Colorado Well #100.

CONCLUSIONS

For simple check shot surveys (small source offset, large observation intervals) elementary velocity analysis techniques are often adequate. However, as more complex VSP surveys are performed and from which more information is expected, increasingly sophisticated analysis techniques are required.

Trial and error ray tracing for velocity or the integral method can produce reasonable results in data sets with low noise. However, the procedure is operator-intensive, can sometimes give erroneous velocities and does not provide an indication of the quality of the solution.

The linear inverse method (Levenberg–Marquardt) solves some of these problems through the use of the damped least-squares criterion. Synthetic results demonstrate the accuracy and stability of the algorithm. Three field VSP surveys analyzed here show the type of resolution and confidence that may be achieved with the linear inverse. VSP velocities appear to be slightly lower than those obtained from the sonic log. The VSP is able to delineate several thin gas zones due to their velocity anomalies. An accurate depth of specific lithology changes in the ENIX, Gulf Coast and Colorado field data has been determined using the velocity variation as computed by the inverse procedure.

Acknowledgments

The author wishes to express his appreciation to the ARCO Oil and Gas Company, Dallas, Texas, for releasing much of the data used in this paper. Dr Stewart was employed by ARCO Oil and Gas Co. for a period during which part of this work was completed and he is grateful for the many discussions with their VSP group.

Appendix A

Intuitively, it is expected that the accuracy of a first-break pick on a seismogram will be related to the frequency of the arrival f_m and the signal-to-noise ratio (S/N).

Aki and Richards (1980) have given a formula to quantify the above intuitions. They suggest that the time-picking error Δt is as follows:

$$\Delta t = \frac{1}{f_m \log_2 [1 + (S/N)^2]}. \tag{A1}$$

The signal-to-noise ratio for a first break is difficult to define. Aki and Richards (1980) empirically determined that the RMS amplitude S should be set equal to 1/20 of the maximum height of the arrival. N is the standard RMS amplitude of the noise.

Suppose, for example, that $f_m = 100$ Hz and $S/N = 3$, then $\Delta t = 3$ ms. This value is probably realistic for a single seismogram but perhaps too large for the hand-picked VSP case, as there is some type of eye correlation between VSP traces at consecutive depths which gives a pick with less error.

Appendix B

Suppose (after Thurber 1981) that the ray-traced traveltimes t^i_{cal}, for the ith depth have been calculated for some velocity model. The traveltime residual is defined by

$$r^i = t^i_{\text{obs}} - t^i_{\text{cal}}, \qquad i = 1, M, \tag{B1}$$

where t^i_{obs} is the observed traveltime at depth i, and M is the total number of observations.

The goal is to perturb the model velocities v_j, such that the resulting change in the calculated traveltime $\Delta t^i_{\mathrm{cal}}$, will make r^i small:

$$t^i_{\mathrm{obs}} - t^i_{\mathrm{cal}} - \Delta t^i_{\mathrm{cal}} \approx 0, \qquad i = 1, M. \tag{B2}$$

Equation (B2) will never be exactly zero for all i because of errors in the traveltime data and model. Combining (B1) and (B2) gives

$$r^i \approx \Delta t^i_{\mathrm{cal}}. \tag{B3}$$

Next expand t^i_{cal} in a Taylor series and truncate it after the first term (the linearity assumption)

$$\Delta t^i_{\mathrm{cal}} = \sum_{j=1}^{n} \frac{\mathrm{d}t^i_{\mathrm{cal}}}{\mathrm{d}V_j} \Delta V_j, \qquad i = 1, M \tag{B4}$$

$$\Delta t^i_{\mathrm{cal}} = t^i_{\mathrm{cal}}(V^1_j) - t^i_{\mathrm{cal}}(V^2_j), \tag{B5}$$

where V^1_j is the first estimated velocity of the jth model layer, V^2_j is the second estimate, N is the total number of layers, and ΔV_j is the required velocity change $(V^1_j - V^2_j)$.

In matrix form, equation (B4) may be written

$$\boldsymbol{Y} = \boldsymbol{A}\boldsymbol{X}, \tag{B6}$$

where $\boldsymbol{Y}$ is a column vector of Δt^i's; $i = 1, M$, $\boldsymbol{X}$ is a column vector of ΔV_j's; $j = 1, N$, and $\boldsymbol{A}$ is the matrix of partial derivatives, $\mathrm{d}t^i_{\mathrm{cal}}/\mathrm{d}V_j$.

As mentioned previously, several problems (including noise) preclude an exact solution to (B6). However, an appeal to the least-squares criterion makes a solution possible. This constraint on (B6) states that the sum of all the squares of the traveltime residuals must be minimized. Thus, the following equations must hold.

$$\frac{\mathrm{d}}{\mathrm{d}V_j} \sum_{i=1}^{M} (r^i)^2 = \frac{\mathrm{d}}{\mathrm{d}V_j} (\boldsymbol{Y}^T\boldsymbol{Y}) = 0; \qquad j = 1, N. \tag{B7}$$

This leads to the least-squares solution,

$$\hat{\boldsymbol{X}} = (\boldsymbol{A}^T\boldsymbol{A})^{-1}\boldsymbol{A}^T\boldsymbol{Y} \tag{B8}$$

For more stability in the solution $\hat{\boldsymbol{X}}$, the damped least-squares technique may be employed (Marquardt 1963, Brown and Dennis 1972). The solution is then given by

$$\boldsymbol{X} = (\boldsymbol{A}^T\boldsymbol{A} + \lambda^2\boldsymbol{I})^{-1}\boldsymbol{A}^T\boldsymbol{Y}, \tag{B9}$$

where λ^2 is the damping parameter.

The damping parameter λ^2 is related to the variance of the data and the variance of the solution. In the present formulation, it is assumed that the observations all have the same variance, and that the velocities are uncorrelated. The algorithm continues to iterate until the Δt_{cal} are within the assumed traveltime error or the new velocity estimate is negligibly different from the previous estimate. There are two statistical estimations that are born out of this formulation. The resolution matrix $\boldsymbol{R}$ gives the relationship between the unattainable true solution $\boldsymbol{X}$, and this estimate of it, $\hat{\boldsymbol{X}}$:

$$\hat{\boldsymbol{X}} = \boldsymbol{R}\boldsymbol{X} = (\boldsymbol{A}^T\boldsymbol{A} + \lambda^2\boldsymbol{I})^{-1}\boldsymbol{A}^T\boldsymbol{A}\boldsymbol{X}. \tag{B10}$$

If $\boldsymbol{R} = \boldsymbol{I}$ or ($\lambda^2 = 0$), then the solution is exactly the true solution (i.e., the resolution is perfect). A numerical smear about the diagonal of $\boldsymbol{R}$ indicates that the procedure has not been able to give completely separate estimates of the parameters (i.e., there are too many velocity layers).

The covariance matrix $\boldsymbol{C}$ of the parameter changes, may be used to estimate the standard deviation of the parameters (velocities):

$$\boldsymbol{C} = (\Delta\boldsymbol{X}\Delta\boldsymbol{X}^T) = \sigma^2(\boldsymbol{A}^T\boldsymbol{A} + \lambda^2\boldsymbol{I})^{-1}\boldsymbol{R}^T, \tag{B11}$$

where $\boldsymbol{R}$ is the resolution matrix, σ^2 is the variance of the data, and $\Delta\boldsymbol{X}$ is the parameter error vector.

References

Aki, K. and Richards, P.G. 1980, Quantitative Seismology: Theory and Methods, V. II, W.H. Freeman Co., San Francisco, CA.

Balch, A., Lee, M.W., Miller, J.J. and Ryder, R.T. 1982, The use of vertical seismic profiles in seismic investigations of the Earth, Geophysics 47, 906–918.

Beeston, H.E. and McEvilly, T.V. 1977, Shear wave velocities from downhole measurements, Earthquake Engineering and Structural Dynamics 5, 181–190.

Brown, K.M. and Dennis, J.E. 1972, Derivative free analogues of the Levenberg–Marquardt and Gauss algorithms for nonlinear least-squares approximation, Numerical Mathematics 18, 289–296.

Crosson, R.S. 1976, Crustal structure modelling of earthquake data: simultaneous least-squares estimation of hypocenter and velocity parameters, Journal of Geophysical Research 81, 3036–3046.

Devaney, A.J. 1982, Geophysical diffraction tomography, submitted to IEEE Transactions, Geological Sciences.

Dix, C.H. 1945, The interpretation of well-shot data II, Geophysics 10, 160–170.

Dix, C.H. 1981, Seismic Prospecting for Oil, 2nd edition, International Human Resources Development Corporation, Boston, MA.

Domenico, S.N. 1977, Elastic properties of unconsolidated porous sand reservoirs, Geophysics 42, 1339–1368.

Flinn, E.A. 1960, Local earthquake location with an electronic computer, Bulletin of the Seismological Society of America 50, 467–470.

Gal'perin, E.I. 1974, Vertical Seismic Profiling, Society of Exploration Geophysicists, Special Publication No. 12, Tulsa, Okla., (originally published in Russian by Nedra, Moscow, USSR, 1971).

Gamburtsev, A.G. 1969, Determining velocity characteristics of a medium using well shooting with observation points inside the medium, Exploration Geophysics 99 (trans. of Prikladnaya Geofiz. 49, 45–58, in Russian).

Ganley, D.C. and Kanasewich, E.R. 1980, Measurement of absorption and dispersion from check shot surveys, Journal of Geophysical Research 85, 5219–5226.

Goetz, J.F., Dupal, L. and Bowles, J. 1979, An investigation into the discrepancies between sonic log and seismic check shot velocities, Australian Petroleum Exploration Association Journal 19, 131–141.

GRANT, F.S. and WEST, G.F. 1965, Interpretation Theory in Applied Geophysics, McGraw Hill Co., N.Y.

GREGORY, A.R. 1977, Aspects of rock physics from laboratory and log data that are important in seismic interpretation, *in* Seismic Stratigraphy—Applications to Hydrocarbon Exploration (ed. C.A. Payton), AAPG Memoir Publication 26, Tulsa, OK.

HARDAGE, B.A. 1983, Vertical Seismic Profiling, Part A: Principles, Geophysical Press, London.

KENNETT, P., IRESON, R.L. and CONN, P.J. 1980, Vertical seismic profiles: Their application in exploration geophysics, Geophysical Prospecting 28, 679–699.

LASH, C.C. 1980, Shear waves, multiple reflections and converted waves found by deep vertical wave test (vertical seismic profile), Geophysics 45, 1373–1411.

MARQUARDT, D.W. 1963, An algorithm for least-squares estimation of non-linear parameters, Journal of the Society of Industrial Applied Mathematics 11, 431–441.

MIT/CGG. 1983, Vertical seismic profiling: A reservoir delineation study, Research Proposal, Cambridge, MA.

O'DOHERTY, R.F. and ANSTEY, N.A. 1971, Reflections on amplitudes, Geophysical Prospecting 19, 430–458.

RICE, R.B., ALLEN, S.J., GANT, JR, O.J., HODGSON, R.N., LARSON, D.E., LINDSEY, J.P., PATCH, J.R., LAFEHR, T.R., PICKETT, G.R., SCHNEIDER, W.A., WHITE, J.E. and ROBERTS, J.C. 1981, Developments in exploration geophysics, 1975–1980, Geophysics 46, 1088–1099.

SCHOENBERGER, M. and LEVIN, F.K. 1978, Apparent attenuation due to intrabed multiples II, Geophysics 43, 730–737.

STEWART, R.R. 1983, Vertical seismic profiles: The one-dimensional forward and inverse problems, PhD Thesis, Department of Earth and Planetary Sciences, Cambridge, MA.

STEWART, R.R., HUDDLESTON, P.D. and KAN, T.K. 1983, Seismic versus sonic velocity: a vertical seismic profiling study, Geophysics (in press).

STEWART, R.R., TURPENING, R.M. and TOKSÖZ, M.N. 1981, Study of a sub-surface fracture zone by vertical seismic profiling, Geophysical Research Letters 8, 1132–1135.

STRICK, E. 1971, An explanation of observed time descrepancies between continuous and conventional well surveys, Geophysics 36, 285–295.

THURBER, C.H. 1981, Earth structure and earthquake locations in the Coyote Lake area, central California, PhD Thesis, Department of Earth and Planetary Sciences, M.I.T., Cambridge, MA., pp. 332.

WIGGINS, R.A. 1972, The general linear inverse problem: Implication of surface waves and free oscillations for earth structure, Review of Geophysics and Space Physics 10, 251–285.

WUENSCHEL, P.C. 1965, Dispersive body waves—an experimental study, Geophysics 30, 539–551.

ZEITVOGEL, M.E. 1982, Investigation of frequency dependent attenuation in a vertical seismic profile, MS Thesis, Graduate College, Texas A & M University, College Station, TX.